Dynamics of vibrationally mediated photodissociation of CH_3CFCl_2

Tina Einfeld, Christof Maul, and Karl-Heinz Gericke
Institut für Physikalische und Theoretische Chemie, Technische Universität Braunschweig, Hans-Sommer-Straße 10, D-38106 Braunschweig, Germany

Ran Marom and Salman Rosenwaks
Department of Physics, Ben-Gurion University of the Negev, Beer-Sheva 84105, Israel

Ilana Bar
The Institutes for Applied Research, Ben-Gurion University of the Negev, Beer-Sheva 84105, Israel

(Received 8 June 2001; accepted 30 July 2001)

The ~235 nm photodissociation of CH_3CFCl_2 pre-excited to three, four, and five quanta of C–H methyl stretches was studied to investigate the effect of internal parent excitation on the dynamics of two- and three-body photofragmentation. The ~235 nm photons also tagged spin-orbit ground $Cl\,^2P_{3/2}$ [Cl] and excited $Cl\,^2P_{1/2}$ [Cl*] state photofragments, via (2+1) resonantly enhanced multiphoton ionization in a time-of-flight mass spectrometer. Monitoring the shapes of ^{35}Cl and $^{35}Cl^*$ time-of-arrival profiles revealed their energies and angular distributions and showed broad and unstructured fragment kinetic energy distributions. Although a significant amount (~50%) of the available energy is transferred into internal energy of the CH_3CFCl fragment, the spatial Cl distribution is characterized by a nonvanishing anisotropy parameter, β, which indicates at a fast dissociation of the parent molecule along the C–Cl dissociation coordinate. Moreover, β for Cl changes from a slightly positive value to a negative value, while that for Cl* increases when the pre-excitation is increased from three to five quanta of C–H methyl stretches. This is attributed to the promotion of one of the nonbonding electrons located on the Cl atoms to the σ^* antibonding C–Cl orbital and involvement of several upper states with different symmetry properties. © *2001 American Institute of Physics.* [DOI: 10.1063/1.1404392]

I. INTRODUCTION

The hydrochlorofluorocarbons (HCFC's) have reached a fundamental significance since they were introduced as interim replacements for chlorofluorocarbons (CFC's), that release atomic chlorine into the stratosphere, which participates in the catalytic ozone destruction cycle. Consequently, photochemistry of the HCFC's is placed in the focus of the attention of atmospheric chemists in order to evaluate the HCFC ozone depletion potential.[1] The interest in HCFC photodissociation is normally linked to fragmentations into two photoproducts. However, at higher dissociation energies, conditions that might be found in the upper stratosphere, three-body decay, where molecules split into three photofragments becomes possible and needs to be taken into account for an understanding of atmospheric chemistry.

Apart from its role in atmospheric processes, the dynamics of three-body decay has recently become a subject of research in its own right.[2,3] Nevertheless, until today, even for photoinduced three-body decay, as the simplest example of an elementary three-body chemical process, only few studies exist, leaving an almost unexplored field of chemical reaction dynamics. In particular, studies that test the effect of initial parent nuclear motion on three-body fragmentation are scarce.[4] Although of high complexity, they can provide new insight into these processes and an understanding of bond breaking. Of particular interest in three-body dissociation is the energy disposal among the emerging fragments and their spatial distribution that might shed light on the involved potential energy surfaces (PES's) and the ensuing dynamics during dissociation.

Vibrationally mediated photodissociation (VMP),[5,6] in which molecules are prepared in a vibrationally excited state and then promoted by a photon to a dissociative excited state, is now recognized as a method that provides direct means for studying the influence of rovibrational excitation on dynamics. The VMP approach was applied to the two-body fragmentation of several molecular systems including hydrocarbons.[4,7–15] These studies revealed the effect of the initial state preparation on relative yields of product channels, internal state distributions, and vector correlations. In particular, in some cases alteration of product identity or distribution in VMP could be found in comparison to the almost isoenergetic one-photon photodissociation.[7,8,11–14] This is due to sampling of different portions of the upper PES by the vibrationally excited wave function and to the participation of more than one PES, leading to different adiabatic and nonadiabatic interplay in VMP compared to the one-photon photodissociation.

Like the impact of vibrational preexcitation on two-body photodissociation, it is expected that three-body breakup of molecules might also be affected by internal nuclear motion of the parent. The feasibility of corresponding experiments has recently been demonstrated by the evidence for the onset of three-body decay in the photodissociation of vibrationally excited $CHFCl_2$.[4]

Halogenated alkane compounds containing two identical

halogen atoms are ideal candidates for studying three-body decay. Their electronic configuration lets one expect a localized electron excitation from nonbonding electrons located on the halogen (X) atoms into the antibonding σ^* (C–X) orbital,[16] thus weakening both C–X bonds simultaneously and leading to their rupture. Three-body decay has been studied in detail for CF_2Br_2[17] and CF_2I_2,[18] which exhibit easily accessible absorption bands above 200 nm and a relatively low three-body decay threshold. For CF_2Br_2, a sequential three-body decay was observed in the wavelength range from 260 to 223 nm, whereas for CF_2I_2 a smooth transition took place from a two- to a concerted three-body decay, in competition with two additional I_2 producing channels, upon increasing the energy of the dissociating photon from 3.53 eV (351 nm) to 6.42 eV (193 nm).

Vibrationally mediated photodissociation studies are greatly facilitated by the existence of chemical bonds where a significant amount of energy can be deposited upon vibrational excitation. To this end, one or more C–H, O–H, or N–H bonds are employed to tune the pre-excitation energy over a wide range. In our study of the VMP of $CHFCl_2$[4] the evidence for the onset of three-body decay was observed upon surpassing the three-body decay threshold by increasing the energy of the vibrational pre-excitation of the C–H bond. The VMP of $CHFCl_2$ pre-excited to the 3_1 and 4_1 C–H polyad components occurs via two-body decay, while that of $CHFCl_2$ (5_1) occurs via both two- and three-body decay. The three-body decay mechanism cannot unequivocally be determined due to the little available energy in the decay to three fragments. Nevertheless, the observed anisotropy parameter, β, of 0.47 for ground state $Cl\,^2P_{3/2}$ [Cl] atoms, suggests a concerted decay in agreement with the expectations from considering the involved molecular orbitals (MO's). Yet, observation of different β values, accompanied by different kinetic energy distributions (KED's) for the spin-orbit states of the chlorine atoms, are an evidence of a more complex fragmentation scheme involving excited states of A' and A'' symmetries that probably mix via curve crossing.

Like $CHFCl_2$, we have recently studied the ~235 nm photodissociation of jet-cooled CH_3CFCl_2 excited with two and three quanta of C–H methyl stretches.[14] The action spectra and the Doppler profiles of the corresponding photofragments were measured, revealing that both Cl and $Cl\,^2P_{1/2}$ [Cl*] are released as a result of C–Cl bond cleavage. The action spectra were characterized by a multiple peak structure, attributed, relying on a simplified local mode model,[19,20] to couplings of C–H methyl stretches and deformations. From the area ratios of the Doppler profiles, the Cl*/Cl branching ratio was found to be ~0.5.

In this paper, in continuation of our work on $CHFCl_2$[4,15] and on direct photodissociation of CH_3CFCl_2[21] at 193 nm, we report on the results of ~235 nm photodissociation of CH_3CFCl_2[13,14] excited with three, four, and five quanta of C–H methyl stretches.[14,20] This molecule was chosen to study the involvement of the different PES's, to examine the role of the three-body channel in VMP and to get insight on the structural dependence of the decay mechanism. The speed distribution $f(v)$ and anisotropy parameters, β, were obtained from the time-of-arrival profiles of ^{35}Cl and $^{35}Cl^*$. The energy distributions of both Cl and Cl* for molecules prepared in the $\nu_{C-H}=3-5$ C–H methyl stretches of CH_3CFCl_2 are broad and similar, ranging from nearly zero center-of-mass (c.m.) translational energy to the maximal available energy. Therefore, it seems that the energy remains mainly in the parent fragment CH_3CFCl where the internal energy increases with pre-excitation from three quanta of C–H methyl stretches to five. Nevertheless, the energy distribution of Cl obtained via five quanta of C–H methyl stretches differs from that via three or four quanta states by a tail in the lower energy region. The small fraction of ''slow'' photofragments indicates an onset of a three-body channel for the photodissociation via five quanta of methyl stretches where the three-body decay threshold is surpassed. For spin-excited Cl*, no hint for a three-body decay was observed.

II. EXPERIMENT

The experiments were carried out in a home-built Wiley–McLaren TOFMS[22] similar to that reported previously.[13–15] The CH_3CFCl_2 sample (98% purity), prepared as a ~10% mixture in Ar at a total pressure of 10^3 mbar, was expanded through a nozzle-skimmer arrangement. The pressure in the ionization chamber was typically $\sim 8\times10^{-6}$ mbar under working conditions. The beam is characterized by a rotational temperature of ~8 K and a vibrational temperature of <100 K, as estimated from the VMP of propyne-d_3 ($3\nu_1$), carried out under similar conditions.[11] These temperatures minimize the rotational inhomogeneous structure and the overlap with hot bands in the region of the monitored vibrational states.[14] The source of vibrational overtone excitation (IR/visible) pulses, (typically 6 mJ around 1166.3 nm for preparation of $\nu_{C-H}=3$, 10 mJ around 887.4 nm for $\nu_{C-H}=4$, and 12 mJ near 727 nm for $\nu_{C-H}=5$) was the idler beam of an optical parametric oscillator (bandwidth ~0.08 cm^{-1}). Following the excitation pulse, after a delay of typically 15 ns, the excited CH_3CFCl_2 molecules were photodissociated by a counterpropagating UV beam (ca. 120 μJ) from a frequency doubled tunable dye laser (~0.4 cm^{-1}). The wavelength of this beam was chosen to fit the two-photon transition of Cl ($4p\,^2D_{3/2}\leftarrow 3p\,^2P_{3/2}$) at 235.336 nm and Cl* ($4p\,^2P_{1/2}\leftarrow 3p\,^2P_{1/2}$) at 235.205 nm to tag the photofragments by (2+1) REMPI.[23] The IR/visible beam was focused with a 15 cm focal length (f.l.) lens and the photolysis/probe (UV) beam with a 30 cm f.l. lens. The UV laser photolyzed the CH_3CFCl_2 molecules efficiently only when overtone excitation was induced, due to the very low absorption cross section of vibrationless ground-state molecules at 235 nm.[24]

Ions formed via REMPI in the focal volume were subjected to continuously biased extraction (−450 V), two acceleration stages (−850 V and −1700 V), two pairs of orthogonal deflection plates, and an einzel lens prior to entering the field-free drift region and eventual detection by a microsphere plate. The time-of-arrival profiles of the ^{35}Cl and $^{35}Cl^*$ resulting from 5000 shots were recorded with a digital oscilloscope and stored on a disk for later analysis. The TOF profiles were taken under space focusing

conditions[22] at two different geometries, vertical (UV laser polarization perpendicular to the TOF axis) and horizontal (UV laser polarization parallel to the TOF axis). The effect of the apparatus on the time-of-arrival profiles was previously determined[4] using the approach of Varley and Dagdigian,[25] i.e., measurement of the time-of-arrival profiles of ^{35}Cl photofragments from 355 nm photolysis of Cl_2. These profiles allowed the electric field strength, E, to be calculated in the ionization region, which was found to be 124 V/cm, 12% lower than the nominal field strength. In addition, the profiles enabled the estimation of the apparatus response time and the effective probe laser linewidth that affects the time-of-arrival profiles through Doppler velocity selection along the probe laser direction.[25]

The KED's and the anisotropy parameter were extracted from the TOF profiles, employing a previously described forward convolution method.[4]

III. RESULTS AND DISCUSSION

A. Time-of-arrival profiles and their analysis

Experimental ^{35}Cl and $^{35}Cl^*$ ion arrival profiles, following the ~235 nm photodissociation of CH_3CFCl_2 prepared in the main peak of the observed multiple peak structure of $\nu_{C-H}=3-5$ vibrational states[14,20] are displayed in Figs. 1(a)–1(c), respectively. In the case of four quanta of C–H methyl stretches, the pre-excitation of the two main peaks observed in the action spectra[20] were examined, whereas for $\nu_{C-H}=3$ and 5, only the main peak was measured. No significant differences were found between the two in $\nu_{C-H}=4$, therefore only the results from the main peak are presented. Although essentially similar distributions were observed, at slightly longer flight times, for the ^{37}Cl fragments, only the portions showing the ^{35}Cl fragments are exhibited. Also, since the intensity of the signal of ^{35}Cl is three times larger than that of ^{37}Cl, due to its larger natural abundance, analysis of the former was preferred. These profiles represent the VMP "net" profiles, and were obtained by removing the small contribution, when present, resulting from the ~235 nm photodissociation of vibrationless ground-state molecules (vibrational excitation laser off) from the signal monitored when both the vibrational excitation laser and the UV laser were on.

The observed profiles were obtained with the polarization of the photolysis/probe UV laser parallel or perpendicular to the TOFMS axis and with the polarization of the IR/visible vibrational excitation laser axis remaining fixed with perpendicular polarization. The profiles of both Cl and Cl*, taken under these polarization conditions, are shown in Figs. 1(a)–1(c).

The main feature in the profiles of Fig. 1 is found in the difference between the shapes of the Cl and Cl* spin-orbit components. The ground-state Cl photofragment spectra are singly peaked for the parallel and perpendicular polarization of the UV laser, although different widths and profile shapes are noticeable for different UV polarization. The excited state Cl* photofragment spectra are doubly peaked for the parallel and singly peaked for the perpendicular polarization of the UV laser. The profiles obtained for the pre-excitation

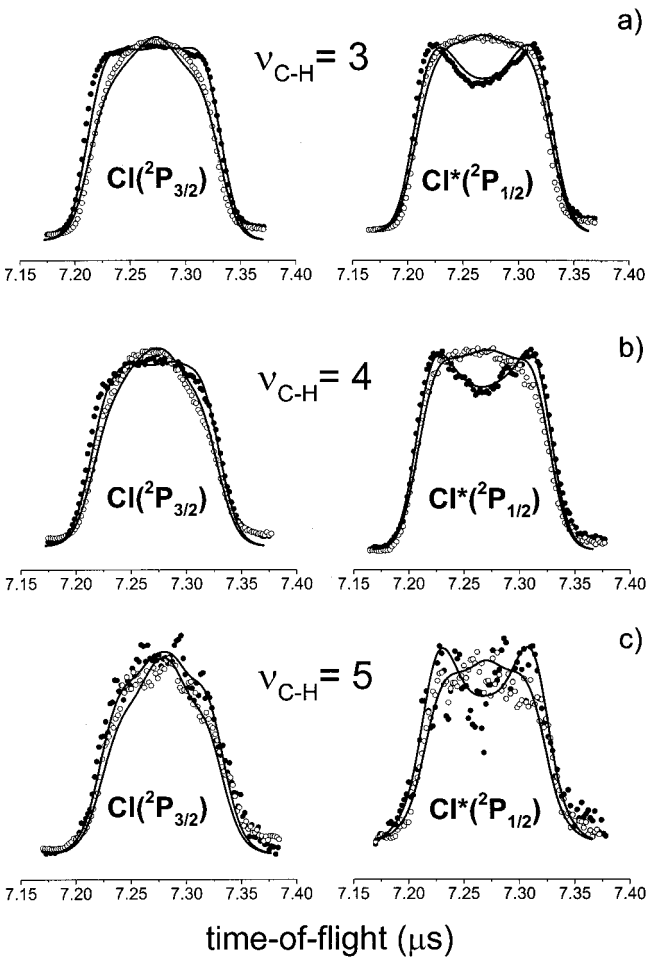

FIG. 1. Arrival time distributions of $^{35}Cl(^2P_{3/2})$ and $^{35}Cl(^2P_{1/2})$ photofragments produced in the ~235 nm photolysis of CH_3CFCl_2 pre-excited with three quanta (panel a), four quanta (panel b), and five quanta (panel c) of C–H methyl stretches. Solid points and open circles are the experimental data points taken with the polarization of the UV photolysis/probe laser parallel and perpendicular, respectively, to the TOFMS axis. The polarization of the overtone excitation laser was perpendicular to the TOFMS axis. Solid lines are the simulations of the corresponding profiles. These lines denote the best-fit velocity distributions, with constant β, finite time response of the apparatus (modeled as a Gaussian with 20 ns full-width-half-maximum) and Doppler selection by the finite bandwidth of the probe laser (modeled as 0.3 cm^{-1} at the 1-photon wave number).

of five quanta of C–H methyl stretches are noisier than that of $\nu_{C-H}=3$ and 4 due to the smaller transition probability in the vibrational excitation step, but the qualitative behavior remains the same. A doubly peaked TOF profile is observed only if the dissociation process forms photofragments of equal translational energies but with velocity vectors pointing toward and opposite the flight axis. These spatially anisotropic fragment distributions are characterized by relatively narrow speed distributions, $f(v)$, centered around a large speed value $\overline{v}$. In principle, ion-flyout, where particles miss the detector because of small velocity components v_z towards the detector and large velocity components perpendicular to the detector axis would also reduce the profile center, but the acceleration voltages were adjusted so that this effect can be ruled out.

The spatial fragment distribution $P(v\theta) \propto f(v)(1+\beta(v)P_2(\cos\theta))$[26,27] is characterized by the velocity depen-

dent anisotropy parameter β ranging from -1 (perpendicular transition) to $+2$ (parallel transition), where θ is the angle of the polarization vector of the dissociating laser with the product recoil velocity vector, and P_2 is the second Legendre polynomial: $P_2(x)=\frac{1}{2}(3x^2-1)$. The observed difference in the profile shapes of the different spin-orbit states could, in principle, be accounted for by a similar speed distribution accompanied by a significantly different anisotropy parameter. However, the calculated β parameter does not vary significantly for Cl and Cl* in $\nu_{C-H}=3$ and 4 pre-excitation (see Sec. III C).

Therefore, the increase in the intensity of the center of the arrival time distribution obtained in VMP of CH_3CFCl_2 $\nu_{C-H}=3-5$ can be attributed to an increase in production of ground-state Cl photofragments with nearly zero center-of-mass (c.m.) translational energies. The difference in the profile shapes for perpendicular and parallel polarization geometries in the case of pre-excitation of $\nu_{C-H}=3$ and 4 indicates that both Cl and Cl* photofragments are released predominantly through a parallel electronic transition with a positive β.[26,28,29]

To quantitatively extract the β parameters and the c.m. Cl and Cl* photofragment speed distribution, simulations of the TOF profiles were carried out and optimized by a genetic algorithm procedure which minimized the deviation of the simulated profile from the experimentally observed profile. Identical β parameters were used for simultaneously fitting the profiles for both polarization geometries. The simulation procedure has successfully been employed for the dissociation of $CHFCl_2$.[4] The best results for the KED obtained by the simulations are shown in Fig. 2. As can be seen from Fig. 1, the fits to the experimental data are of good quality, although only a single velocity-independent β parameter was employed in the simulation procedure.

B. Energy distributions

The kinetic energy distributions, $P(E)$, and the β parameters obtained for Cl and Cl* photofragments resulting from VMP via three, four, and five quanta of C–H methyl stretches are shown in Figs. 2(a)–2(c). The combined energies (IR/visible+UV) employed in the VMP of CH_3CFCl_2 $\nu_{C-H}=5$ [$\sim$56 240 cm^{-1} (673 kJ/mol)], $\nu_{C-H}=4$ [$\sim$53 760 cm^{-1} (643 kJ/mol)] and $\nu_{C-H}=3$ [$\sim$51 070 cm^{-1} (611 kJ/mol)] exceed that required for the loss of one chlorine atom,

$$CH_3CFCl_2 \xrightarrow{h\nu} CH_3CFCl+Cl \quad (\Delta H^0_{298}=351\pm35 \text{ kJ/mol}), \tag{1}$$

and for the loss of molecular chlorine

$$CH_3CFCl_2 \xrightarrow{h\nu} CH_3CF+Cl_2 \quad (\Delta H^0_{298}=417\pm42 \text{ kJ/mol}), \tag{2}$$

but the pre-excitation via $\nu_{C-H}=3$ and $\nu_{C-H}=4$ does not surpass the threshold for the three-body process where two chlorine atoms are released:

$$CH_3CFCl_2 \xrightarrow{h\nu} CH_3CF+Cl+Cl \quad (\Delta H^0_{298}=660\pm66 \text{ kJ/mol}). \tag{3}$$

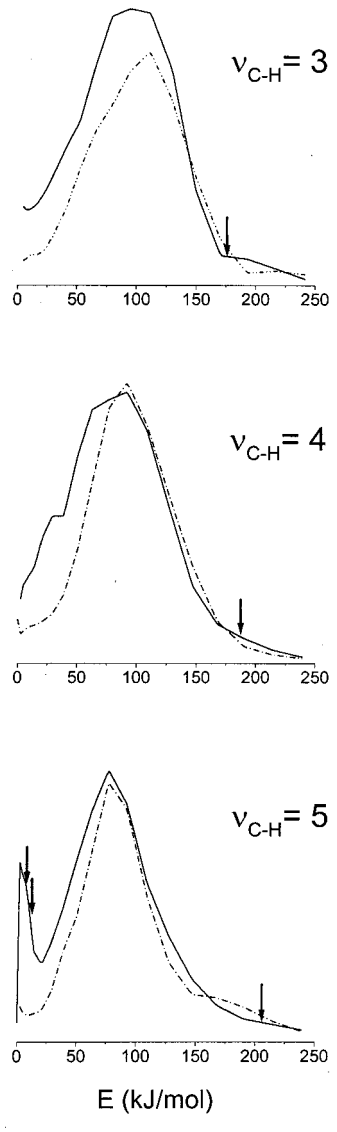

FIG. 2. Energy distributions of $^{35}Cl(^2P_{3/2})$ (solid line) and $^{35}Cl(^2P_{1/2})$ (dashed line) in $\sim$235 nm photodissociation of vibrationally excited CH_3CFCl_2 $\nu_{C-H}=3-5$. The distribution was obtained from simultaneous fitting of the parallel and perpendicular profiles. The arrows at the high energies, in the different panels, indicate the maximum possible energies calculated for the two-body photodissociation of $CHFCl_2$ for three, four, and five quanta of C–H methyl stretches, respectively. The other two arrows in the slow energy region of the bottom panel indicate the maximum allowed energy in the sequential and concerted three-body process, respectively.

The enthalpies, ΔH^0, of reactions (1) and (3) were calculated for the spin-orbit states with the lowest energy from the standard enthalpies of formation (ΔH^0_f) of the molecule and radicals involved in the process[30–32] and the errors were calculated as the sum of individual squared errors. The standard enthalpies were partly estimated as arithmetic means from the fully chlorinated and fluorinated species, when data was not available in the literature. The ΔH^0_{298} required for loss of one or two Cl* atoms are higher than the values given for Cl in reactions (1) and (3) by 10.6 kJ/mol and 21.2 kJ/mol, respectively.

Taking into account the combined energies channeled into CH_3CFCl_2 molecules, and assuming that ΔH^0 equals

TABLE I. Calculated maximal kinetic energies E_{max}, observed mean total $\overline{E_T}$, fraction of the kinetic energy and the β anisotropy parameters in the photodissociation of vibrationally excited CH_3CFCl_2.

CH_3CFCl_2		E_{preex} (kJ/mol)	E_{max} (kJ/mol)	$\overline{E_T}$ (kJ/mol)	E_{int} (kJ/mol)	E_T/E_{avl}	β
$\nu_{C-H}=3$	Cl	103	260	119	141	0.46	0.20±0.04
	Cl*		249	131	118	0.53	0.25±0.04
$\nu_{C-H}=4$	Cl	135	292	112	180	0.38	0.20±0.03
	Cl*		281	126	155	0.45	0.25±0.05
$\nu_{C-H}=5$	Cl	165	322	106	216	0.33	−0.14±0.05
	Cl*		311	123	188	0.40	0.35±0.06

the C–Cl bond dissociation energy D_0, the available energy E_{avl} and the maximum energetically allowed energies for Cl photofragments were calculated and are shown in Table I. The maximal kinetic energies for Cl and Cl* arising from decay channel (1) are indicated by the arrows in Fig. 2. In fact, the arrows should be shifted to somewhat larger energies if (ΔH_0^0) are retrieved. The energy distributions are centered at relatively high values with tails that reach the maximum Cl energy as Fig. 2 clearly shows. The correspondence of the distribution centers to large energies might indicate that the dissociation process occurs on a repulsive PES, as expected from the broad and unstructured first absorption band of CH_3CFCl_2.[24]

In addition, the average translational energy E_T release of the $CH_3CFCl+Cl$ fragment pair via reaction (1) is calculated. Since the excess energy E_{avl} is known, the translational energy disposal fraction E_T/E_{avl} can be calculated and is shown in Table I for the different quanta of C–H methyl stretches. In order to compare these values with the recently obtained data for the VMP of $CHFCl_2$,[4] a detailed, second table (Table II) is presented. From estimating the energy release via the impulsive model[33] a value between 0.4 and 0.5 is obtained for E_T/E_{avl} and therefore the measured values seem to be reasonable. Comparison of these values to those for VMP of $CHFCl_2$ (3_1) and (4_1) recently obtained in our group (0.45),[4] and to that obtained by photofragment translational spectroscopy (PTS) experiments of Huber and co-workers[34] in 193 photodissociation (0.44), shows that the values are in good agreement. Our values are also quite close to those measured for the 193 nm photolysis of other chloromethanes releasing Cl photofragments, including: $CHCl_3$ [0.43 (Ref. 34) and 0.41 (Ref. 35)], CF_2Cl_2 [0.50 (Ref. 35) and 0.47 (Ref. 36)], $CFCl_3$ [0.43 (Ref. 35) and 0.47 (Ref. 37)], and CCl_4 [0.35 (Ref. 35)]. This implies that a rather high kinetic energy release occurs in the photodissociation of vibrationally excited CH_3CFCl_2 similarly to the photodissociation of other vibrationless ground-state molecules and of vibrationally excited $CHFCl_2$, agreeing with a direct dissociation process on a repulsive surface. Our results for $CHFCl_2$ and CH_3CFCl_2, and as stated by Huber[34] and Gentry[35] and their co-workers, their translational energy disposal fraction, differ from those obtained by Matsumi *et al.*[38] They probed the Cl atoms by REMPI and measured the Doppler profiles in 193 nm photodissociation of several chloromethanes. The E_T/E_{avl} that they obtained were much higher, i.e., 0.85 for $CHCl_3$ and 0.78 for CH_3Cl. With respect to the latter values, it must be taken into account that an integrative method like Doppler profile analysis generally tends to underestimate the contribution of slow particles, especially if the speed distribution is broad.

It is noteworthy that the $\overline{E_T}$ values shown in Table I remain constant, within experimental error, upon pre-excitation with three to five quanta of C–H methyl stretch. Relying on the involved MO's, the observed anisotropy, and the unstructured absorption spectrum, all hint at a direct, barrierless dissociation on a repulsive surface. Moreover, structurally similar molecules were found to dissociate directly and fast in the dissociation coordinate.[17,34] However, in CH_3CFCl_2 there is no significant additional energy flow into the dissociation coordinate upon increasing C–H methyl stretches excitation as observed in the case of $CHFCl_2$, where $\overline{E_T}$ increased from 126 kJ/mol to 139 kJ/mol upon pre-excitation via three to four quanta of C–H methyl

TABLE II. Calculated maximal kinetic energies E_{max}, observed mean total $\overline{E_T}$, fraction of the kinetic energy and the β anisotropy parameters in the photodissociation of vibrationally excited $CHFCl_2$.

$CHFCl_2$		E_{preex} (kJ/mol)	E_{max} (kJ/mol)	$\overline{E_T}$ (kJ/mol)	E_{int} (kJ/mol)	E_T/E_{avl}	β
3_1	Cl	104	276	126	150	0.46	0.14±0.05
	Cl*		265	134	131	0.50	0.36±0.06
4_1	Cl	136	308	139	169	0.45	0.27±0.06
	Cl*		297	140	157	0.47	0.43±0.05
5_1	Cl	167	339	131	208	0.39	0.47±0.07
Three-body decay			33	>28[a]	<5	0.85	
	Cl*		328	121	207	0.39	0.34±0.04

[a]The > symbol is due to the unknown E_T of CHF.

stretches. This observation can be explained by the following arguments: As the time period between the pre-excitation and the dissociation is by far long enough for a complete redistribution,[14] which occurs on a subnanosecond time scale, the pre-excitation energy via three, four, and five quanta of C–H methyl stretches will be distributed over the 18 normal modes in the CH_3CFCl_2 molecule.[39] Total equipartitioning of the pre-excitation energy on all vibrational degrees of freedom leads to an additional energy flow of 950, 1250, and 1530 cm^{-1}, respectively, into the C–Cl dissociation coordinate. Therefore, only one or two quanta of C–Cl stretch will be populated taking a typical vibrational quantum of 600 cm^{-1} into acount.[40] The corresponding increase of the kinetic energy of the ejected Cl atoms is so small that it is not observable due to the experimental resolution. Whereas in the case of $CHFCl_2$, a smaller molecule with only 9 normal modes, the increase of the kinetic energy of the Cl atoms from photodissociation of 3_1 to 4_1 is noticeable, while via 5_1 the three-body decay channel starts to contribute by adding low kinetic energy fragments. The observation of constant $\overline{E_T}$ hints at a similar shift for the ground- and excited-state surface in the reaction coordinate by approximately the value of the internal energy of the partner fragment CH_3CFCl or CHFCl, whereas the small additional kinetic energy is induced by only few quanta of C–Cl stretches.[41]

The very slow Cl photofragments, observed in the VMP of CH_3CFCl_2 via five quanta of C–H methyl stretches, might emerge from a synchronous concerted three-body decay, where two C–Cl bonds are broken simultaneously, or from a sequential three-body decay.[2,3] For the former, the maximum allowed Cl velocity is 610 m/s (6.5 kJ/mol) and for the latter 720 m/s (9.1 kJ/mol), as indicated by the corresponding arrows of the bottom panel of Fig. 2. It is noteworthy that the calculated maximum energies, based on the above ΔH^0_{298} values for the reactions, suffer from inaccuracies due to the relatively large uncertainties in the enthalpies of formation. The slow atoms contribute to less than 4% to the total Cl fragments, whereas in the case of $CHFCl_2$ the contribution of the three-body decay channel was about 10%. Thus, the dynamics of the three-body decay cannot be verified. In the case of Cl* no slow atoms were observed, which is not surprising due to the very small available energy which would lead to maximal speeds of 270 m/s (1.3 kJ/mol).

C. Anisotropies

The electronic configuration of the ground state is:

$$\ldots(17a')^2(10a'')^2(11a'')^2(18a')^2(12a'')^0(19a')^0.$$

Both unoccupied $(12a'')^0$ and $(19a')^0$ MO's are C–Cl antibonding. The occupied $(17a')^2$, $(10a'')^2$, $(11a'')^2$, and $(18a')^2$ are nonbonding MO's composed of the $3p$-electrons of the Cl atoms. Single electron excitation gives rise to eight states of A' and A'' symmetry which are the result of electron excitation from nonbonding electrons located on the Cl atom into antibonding C–Cl MO's (σ^*(C-Cl)←n(Cl)) leading to a direct decay.

The magnitude and sign of β are related to the symmetry of the ground and excited state, the orientation of the transition dipole moment $\boldsymbol{\mu}$ in the parent molecule and the excited-state lifetime. The theoretical limit for the β parameter, with $\boldsymbol{\mu}$ parallel to the line connecting the two Cl atoms, is estimated to be ~1.1 for the transition $A''\leftarrow A'$ (based on a Cl–C–Cl bond angle of 112° in CH_3CFCl_2) and in the range from −1 to 0 for the transition $A'\leftarrow A'$ as the CH_3CFCl_2 molecule belongs to the C_s symmetry group.

The recoil anisotropies provide essential information regarding the mechanism of bond breaking. The β parameters extracted from the experimental data are shown in Table I. Errors were calculated from the scattering of the 10 "best" β parameters obtained by the data analysis procedure described previously. Relying on the data in Table I, it is seen that the Cl and Cl* arising from ~235 nm photodissociation of CH_3CFCl_2 $\nu_{C-H}=3$ and $\nu_{C-H}=4$ via two-body processes (1) possess positive anisotropies with almost constant values, lower than the limiting values.

The β values obtained in the VMP experiment via $\nu_{C-H}=3$ and $\nu_{C-H}=4$ are positive, ruling out a pure $A'\leftarrow A'$ excitation, however, they are lower than the limiting values for the pure $A''\leftarrow A'$ transition. Relying on the direct excitation of C–Cl antibonding MO's, the dissociation should be prompt and it does not seem likely that the rotational motion accounts for the reduction of β from its limiting value. If only rotation of the parent molecule[42] is responsible for the reduction of β, then lifetimes of $\tau=172$, 57, and 32 fs are estimated for temperatures of 10, 100, and 300 K, respectively, and an equilibrium bond angle of 86°. These small limiting lifetimes are a consequence of the large moments of inertia for the CH_3CFCl_2, leading to fast loss of anisotropy due to molecule rotation. Thus, for a bulk experiment at 300 K, it should be virtually impossible to observe the limiting β parameter values even for a direct decay. Under molecular beam conditions, ($T_{rot}=10$ K, $T_{vib}=100$ K) however, a significantly higher β parameter than the observed values of 0.2 to 0.3 would be expected for a direct fragmentation process. Consequently, the observation of less than limiting β values should emerge from dynamical factors or from the simultaneous excitation of A' and A'' states, that probably mix via curve crossing and release both photofragments. From the measured β and the spin-orbit state branching ratio,[14] it is inferred that both Cl and Cl* in $\nu_{C-H}=3$ and $\nu_{C-H}=4$ photodissociation are produced as a result of simultaneous absorption to A'' and A' states.

Due to the decrease of β corresponding to Cl via $\nu_{C-H}=5$, it is likely that the contribution of an additional excited state of A' symmetry increases. If this involved A' state responsible for the observed β value were identical to the above-mentioned A' state, which releases predominantly Cl* atoms, an increase in the Cl*/Cl branching ratio would be expected. However, a decrease was found in this ratio from 0.36 to 0.16 upon increasing the dissociation energy from 235 nm to 193 nm,[14,21] whereas the ratio is about 0.5 via 235 nm photodissociation pre-excited with three and four quanta of methyl stretches. Therefore it seems that at least three different upper states are involved in the CH_3CFCl_2 photolysis in the 40 000–56 000 cm^{-1} energy range.

The contribution of the three-body decay is small (<4%) although after populating the antibonding σ^* (C–Cl) orbital for both Cl's one would expect significant three-body decay since the energy threshold is surpassed. The insignificant contribution is probably due to the small available energy for the three-body decay. For $CHFCl_2$ evidence of the onset of three-body decay was observed upon surpassing the energetic threshold as a consequence of the larger vibrational excitation of the dissociation coordinate.

In view of the above-discussed MO's, a participation of the molecular channel ($CH_3CFCl_2+h\nu\rightarrow CH_3CF+Cl_2$) is unlikely. Although the $19a'$ MO is antibonding in both C–Cl bonds, the $Cl(3p)$ atomic orbitals contributing to the $19a'$ MO of CH_3CFCl_2 do not correlate to the ground-state Cl_2 σ-bond for the formation of a stable Cl_2 molecule.

All in all the pre-excitation seems to be insignificant for the energetics, but very important for the involvement of the upper states leading to a different spin-orbit branching ratio relative to 193 nm photodissociation of vibrationless ground-state CH_3CFCl_2[14] and to an enormous increase in the signal intensity due to the improved Franck–Condon factors and the different upper PES which are accessed.

IV. CONCLUSIONS

The VMP of CH_3CFCl_2 pre-excited with three, four, and five quanta of C–H methyl stretches was studied using the REMPI-TOF technique for the measurement of time-of-arrival profiles of Cl and Cl* photofragments. The data analysis yielded the photofragment energy distributions and the recoil anisotropy parameters. These results suggest that the photodissociation of CH_3CFCl_2 $\nu_{C-H}=3$, 4, and 5 occurs via two-body decay. The upper limit for the contribution of the three-body decay via CH_3CFCl_2 $\nu_{C-H}=5$ is 4% of the total. The $\overline{E_T}$ distributions change only insignificantly upon increasing the excitation energy from three to five quanta hinting at a fast dissociation and a similar shift of both the ground- and excited-state energies with respect to the dissociation coordinate. Most of the excitation energy remains in the partner fragment CH_3CFCl with increasing internal energy.

While the effect of vibrational excitation on the kinetic energy distribution of the fragment is small, spatial fragment distribution, branching ratios, and the signal intensity are significantly affected by the amount of initially deposited vibrational energy. The anisotropy parameters range from -0.2 to 0.3. They are lower than the limiting value of 1.1 for a pure $A''\leftarrow A'$ excitation indicating that both A' and A'' excited states are involved, which mix via curve crossing to release Cl and Cl*. No significantly different behavior was found for Cl and Cl* except for Cl resulting from the photodissociation of CH_3CFCl_2 excited to five quanta of C–H methyl stretch. Most likely, the large combined excitation energy allows accessing an additional A' state, which predominantly correlates to Cl, thus lowering the effective β parameter. In comparison to the measurement of the photodissociation of vibrationally excited $CHFCl_2$, we conclude that the additional methyl group influences the mechanism of the decay. Purely energetic effects due to the increased total (combined) energy become negligible, whereas the modified vibrational wave function of the electronic ground state results in accessing different parts of the upper PES in a basically constant energy range.

ACKNOWLEDGMENTS

The authors are grateful to Dr. A. Melchior and Dr. A. Chichinin for numerous stimulating discussions. This research was supported by the German-Israeli Foundation (GIF) under Grant No. I 0537-098.05/97 and by the James Franck Binational German-Israeli Program in Laser-Matter Interaction. One of the authors (T.E.) gratefully acknowledges the financial support by the Fond der Chemischen Industrie and the Minerva Foundation.

[1] R. P. Wayne, *The Chemistry of Atmospheres*, 2nd ed. (Oxford University Press, Oxford, 1991).
[2] C. Maul and K.-H. Gericke, Int. Rev. Phys. Chem. **16**, 1 (1997).
[3] C. Maul and K.-H. Gericke, J. Phys. Chem. A **104**, 2531 (2000).
[4] X. Chen, R. Marom, S. Rosenwaks, I. Bar, T. Einfeld, C. Maul, and K.-H. Gericke, J. Chem. Phys. **114**, 9033 (2001).
[5] F. F. Crim, J. Phys. Chem. **100**, 12725 (1996), and references therein.
[6] I. Bar and S. Rosenwaks, Int. Rev. Phys. Chem. (in press), and references therein.
[7] E. Woods III, H. L. Berghout, C. M. Cheatum, and F. F. Crim, J. Phys. Chem. A **104**, 10356 (2000); M. J. Coffey, H. L. Berghout, E. Woods III, and F. F. Crim, J. Chem. Phys. **110**, 10850 (1999).
[8] J. Zhang, C. W. Riehn, M. Dulligan, and C. Wittig, J. Chem. Phys. **103**, 6815 (1995).
[9] R. P. Schmid, T. Arusi-Parpar, R.-J. Li, I. Bar, and S. Rosenwaks, J. Chem. Phys. **107**, 385 (1997); R. P. Schmid, Y. Ganot, I. Bar, and S. Rosenwaks, *ibid.* **109**, 8959 (1998).
[10] R. P. Schmid, Y. Ganot, I. Bar, and S. Rosenwaks, J. Mol. Struct. **480–481**, 197 (1999); T. Arusi-Parpar, R. P. Schmid, R.-J. Li, I. Bar, and S. Rosenwaks, Chem. Phys. Lett. **268**, 163 (1997).
[11] X. Chen, Y. Ganot, I. Bar, and S. Rosenwaks, J. Chem. Phys. **113**, 5134 (2000).
[12] H. M. Lambert and P. J. Dagdigian, J. Chem. Phys. **109**, 7810 (1998); H. M. Lambert and P. J. Dagdigian, Chem. Phys. Lett. **275**, 499 (1997); A. Melchior, H. M. Lambert, P. J. Dagdigian, I. Bar, and S. Rosenwaks, Isr. J. Chem. **37**, 455 (1997).
[13] A. Melchior, X. Chen, I. Bar, and S. Rosenwaks, Chem. Phys. Lett. **315**, 421 (1999).
[14] A. Melchior, X. Chen, I. Bar, and S. Rosenwaks, J. Chem. Phys. **112**, 10787 (2000).
[15] A. Melchior, X. Chen, I. Bar, and S. Rosenwaks, J. Phys. Chem. A **104**, 7927 (2000).
[16] M. B. Robin, Can. J. Chem. **63**, 2032 (1985).
[17] M. R. Cameron, S. A. Jones, G. F. Metha, and S. H. Kable, Phys. Chem. Chem. Phys. **2**, 2539 (2000).
[18] E. A. J. Wannenmacher, P. Felder, and J. R. Huber, J. Chem. Phys. **95**, 986 (1991); G. Baum, P. Felder, and J. R. Huber, *ibid.* **98**, 1999 (1993); K. Bergmann, R. T. Carter, G. E. Hall, and J. R. Huber, *ibid.* **109**, 474 (1998); W. Radloff, P. Farmana, V. Stert, E. Schreiber, and J. R. Huber, Chem. Phys. Lett. **291**, 173 (1998); H. A. Scheld, A. Furlan, and J. R. Huber, *ibid.* **326**, 366 (2000).
[19] J. L. Duncan, C. A. New, and B. Leavitt, J. Chem. Phys. **102**, 4012 (1995).
[20] X. Chen, A. Melchior, I. Bar, and S. Rosenwaks, J. Chem. Phys. **112**, 4111 (2000).
[21] A. Melchior, I. Bar, and S. Rosenwaks, J. Chem. Phys. **107**, 8476 (1997).
[22] W. C. Wiley and I. H. McLaren, Rev. Sci. Instrum. **26**, 1150 (1955).
[23] R. Liyanage, Y. Yang, S. Hashimoto, R. J. Gordon, and R. W. Field, J. Chem. Phys. **103**, 6811 (1995).
[24] A. Fahr, W. Braun, and M. J. Kurylo, J. Geophys. Res. **98**, 20467 (1993).
[25] D. F. Varley and P. J. Dagdigian, J. Phys. Chem. **99**, 9843 (1995).
[26] R. N. Zare, Mol. Photochem. **4**, 1 (1972).
[27] M. Mons and I. Dimicoli, J. Chem. Phys. **90**, 4037 (1989).
[28] G. E. Hall and P. L. Houston, Annu. Rev. Phys. Chem. **40**, 375 (1989).
[29] R. J. Gordon and G. E. Hall, Adv. Chem. Phys. **96**, 1 (1996).
[30] M. W. Chase, NIST-JANAF, Thermochemical Tables, 4th Ed., J. Phys.

Chem. Reference Data, Monograph 9, Part I+II (1998).
[31] W. B. DeMore, S. P. Sander, D. M. Golden, R. F. Hampson, M. J. Kurylo, C. J. Howard, A. R. Ravishankara, C. E. Kolb, and M. J. Molina, JPL Publication 92-20 (1992).
[32] S. Y. Chiang, Y. C. Lee, and Y. P. Lee, J. Phys. Chem. A **105**, 1226–1231 (2001).
[33] H. Okabe, J. Chem. Phys. **53**, 3507 (1970); *Photochemistry of Small Molecules* (Wiley-Interscience, New York, 1978).
[34] X. Yang, P. Felder, and J. R. Huber, Chem. Phys. **189**, 127 (1994).
[35] M. D. Nachbor, C. F. Giese, and W. R. Gentry, J. Phys. Chem. **99**, 15400 (1995).
[36] G. Baum and J. R. Huber, Chem. Phys. Lett. **203**, 261 (1993).
[37] P. Felder and C. Demuth, Chem. Phys. Lett. **208**, 21 (1993).
[38] Y. Matsumi, K. Tonokura, M. Kawasaki, G. Inoue, S. Satyapal, and R. Bersohn, J. Chem. Phys. **94**, 2669 (1991); *ibid.* **97**, 5261 (1992).
[39] T. J. Minehardt, J. David Adcock, and R. E. Wyatt, Chem. Phys. Lett. **303**, 537 (1999), and references therein.
[40] L. J. Bellamy, *The Infrared Spectra of Complex Molecules and Advances in Infrared Group Frequencies* (Chapman and Hall, London, 1958 and 1968).
[41] R. Schinke, *Photodissociation Dynamics*, Cambridge Monographs on Atoms, Molecular and Chemical Physics Vol. 1 (Cambridge University Press, Cambridge, 1993).
[42] G. E. Busch and K. R. Wilson, J. Chem. Phys. **56**, 3638 (1972).